ACI MATERIALS JOURNAL TECHNICAL PAPER

Title no. 106-M36

Influence of Aggregate Type and Size on Ductility and Mechanical Properties of Engineered Cementitious Composites

by Mustafa Şahmaran, Mohamed Lachemi, Khandaker M. A. Hossain, Ravi Ranade, and Victor C. Li

This paper presents the results of an investigation on the influence of aggregate type and size on the mechanical and ductility properties of engineered cementitious composites (ECC). ECC is a micromechanically-based designed high-performance fiber-reinforced cementitious composite with high ductility and improved durability due to tight crack width. Standard ECC mixtures are typically produced with microsilica sand (200 μm [0.008 in.] maximum aggregate size). In this study, ECC mixtures containing either crushed dolomitic limestone sand or gravel sand with maximum sizes of 1.19 or 2.38 mm (0.047 or 0.094 in.) were investigated. For each aggregate type and maximum aggregate size, three different ECC mixtures with fly ash/portland cement (FA/C) ratios of 1.2, 2.2, and 4.2 were cast. Specifically, the effects of maximum aggregate size, aggregate type, and FA/C on the uniaxial tensile, flexure, and compressive properties, as well as crack development and drying shrinkage behavior, were experimentally determined. The experimental results show that the ECC mixtures produced with crushed dolomitic limestone sand and gravel sand with higher maximum aggregate sizes exhibit strain-hardening behavior with strain capacities comparable with the standard microsilica sand ECC mixtures, provided that a high FA content is employed in the matrix. For these mixtures, the tensile ductility can maintain 1.96 to 3.23% at 28 days of age, with tensile strengths of 3.57 to 5.13 MPa (0.52 to 0.74 ksi). The use of crushed dolomitic limestone sand and gravel sand can also play the role of drying-shrinkage arrestors in the paste, further improving the material behavior.

Keywords: aggregates; drying shrinkage; engineered cementitious composites (ECC); flexure; tensile.

INTRODUCTION

Through years of practice and experience, concrete has proven to be a suitable material in infrastructure construction. It has been successfully implemented in numerous projects around the world. However, the recently deteriorating condition of the infrastructure in North America and elsewhere has motivated authorities and researchers to seek property enhancements to this material. High-performance fiber-reinforced cementitious composites (HPFRCCs), with their superior resistance to tensile loads and environmental conditions, have become an increasingly promising materials to address the infrastructure deterioration problem. Engineered cementitious composite (ECC) is a special type of HPFRCC designed with micromechanical principles.[1-3] Micromechanical design allows optimization of the composite for high performance, resulting in extreme tensile strain capacity while minimizing the amount of reinforcing fibers, typically less than 2% by volume. Unlike ordinary cement-based materials, ECC strain-hardens after first cracking, similar to a ductile metal, and demonstrates a strain capacity 300 to 500 times greater than normal concrete (Fig. 1). Even at large imposed deformation, crack widths of ECC remain small, less than 60 μm (0.004 in.) (Fig. 1). With intrinsically tight crack width and high tensile ductility, ECC represents a new generation of high-performance concrete material that offers significant potential to naturally resolving the durability problem of reinforced concrete (RC) structures.[4-9]

Aggregates typically occupy an important volume fraction in cement-based materials, and thus have important effects on different aspects of material properties. In addition to their role as economical filler, aggregates help control the dimensional stability of cement-based materials, which may be considered to consist of a framework of cement paste with relatively large shrinkage movements restrained by the aggregate particles. In the presence of fibers in cement-based materials, however, the introduction of aggregates with a particle size larger than the average fiber spacing leads to balling and greater interaction of fibers in the paste between the large aggregate particles, and the effect becomes more pronounced as the maximum size of particles increases.[10] Therefore, the increase in aggregate particles size makes it more difficult to achieve a uniform dispersion of fibers. Generally, the greater the size of aggregate particles, the more clumping and interaction of fibers occurs.[11]

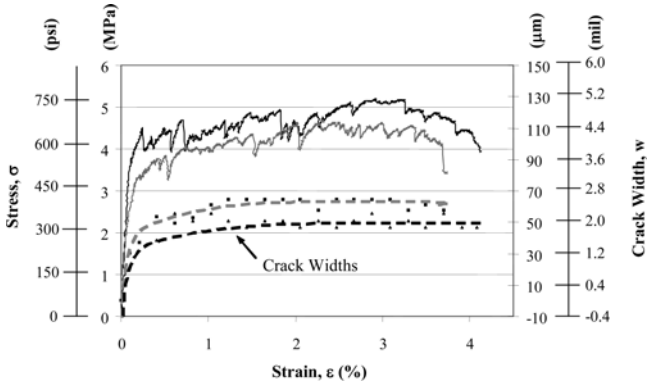

Fig. 1—Typical tensile stress-strain curve and crack width development of ECC.

ACI Materials Journal, V. 106, No. 3, May-June 2009.
MS No. M-2008-299 received September 8, 2008, and reviewed under Institute publication policies. Pertinent discussion including authors' closure, if any, will be published in the March-April 2010 *ACI Materials Journal* if the discussion is received by December 1, 2009.

ACI member **Mustafa Şahmaran** *is an Assistant Professor in the Department of Civil Engineering at the University of Gaziantep, Turkey. He is a member of ACI Committee 237, Self-Consolidating Concrete. His research interests include concrete technology, durability of concrete, and composite materials development for sustainable infrastructure.*

ACI member **Mohamed Lachemi** *is a Canada Research Chair in Sustainable Construction and a Professor in the Department of Civil Engineering at Ryerson University, Toronto, ON, Canada. He is a member of ACI Committee 231, Properties of Concrete at Early Ages, and 237, Self-Consolidating Concrete. His research interests include the use of high-performance materials in the built infrastructure including the development and use of self-consolidating concrete in construction.*

ACI member **Khandaker M. A. Hossain** *is an Assistant Professor in the Department of Civil Engineering at Ryerson University. His research interests include blended cement and concrete, structural application of self-consolidating concrete, composite construction, and finite element analysis of reinforced and composite structures.*

Ravi Ranade *is an MSc Student Research Assistant in the Department of Civil and Environmental Engineering at the University of Michigan, Ann Arbor, MI. He received his BS from the Indian Institute of Technology Bombay, Mumbai, India. His research interests include composite materials development for sustainable infrastructure, and using material methodology for improving durability of civil infrastructure.*

ACI member **Victor C. Li** *is a Professor in the Department of Civil and Environmental Engineering at the University of Michigan. He is a member of ACI Committee 544, Fiber Reinforced Concrete. His research interests include the design of ultra-ductile and green cementitious composites, their application to innovative infrastructure systems, and integration of materials and structural design.*

Moreover, the presence of aggregates in a cement paste matrix tends to increase the tortuosity of the fracture path and, therefore, the matrix fracture toughness.[12,13] The increase in fracture toughness with increasing aggregate particles size is the result of the increased resistance to the propagating crack. Therefore, the size of the aggregate particles is expected to have a significant influence on the fracture properties of the matrix. According to the micromechanical design principles of ECC, to achieve strain hardening, matrix fracture toughness has to be limited such that steady-state crack initiation could occur before the tensile load reaches the maximum fiber bridging stress that would result in failure of the fiber bridges. Large aggregate particles are hence eliminated in the standard ECC mixture as a result of micromechanical-based design calculations. Hence, in spite of positive effects of aggregates on dimensional stability and economy of fiber-reinforced cement composites, there are limits on aggregate particles size beyond which problems with fiber dispersability, fresh mixture workability, and matrix toughness may start to negatively affect the composite material performance characteristics. For these reasons, the production of standard ECC mixtures has been restricted to the use of a fine aggregate such as microsilica sand.

Recently, fly ash (FA) has become what some consider a necessary component of ECC.[4,14,15] Increasing the FA content in ECC mixtures tends to improve robustness of tensile ductility while retaining a long-term tensile strain of approximately 3%. The improvement in the tensile strain with the increase in the FA content can be attributed to the fact that the increase in the FA content tends to reduce the fiber/matrix interface chemical bond and matrix toughness, while increasing the interface frictional bond, in favor of attaining high tensile strain capacity.[14] Because the increase in aggregate size leads to an increase in the matrix toughness, commonly available normal sand with a higher maximum aggregate size could successfully be used in conjunction with high-volume FA in the production of ECC. No information is currently available on the influence of aggregate type and size on the mechanical performance of ECC. Accordingly, the main objective of the current research is to design a new class of ECCs with a matrix incorporating crushed dolomitic limestone sand or gravel sand, and high FA content, that retains the tensile properties of standard ECC mixtures containing microsilica sand.

In this study, several variables were investigated in the production of ECC: 1) three different types of sand (microsilica sand, crushed dolomitic limestone sand, and gravel sand); 2) three different maximum nominal sizes of sand (200 μm [0.008 in.] for the microsilica sand, and 1.19 and 2.38 mm [0.047 and 0.094 in.] for the crushed dolomitic limestone sand and gravel sand); 3) three different FA replacement levels (FA/cement [C] ratio of 1.2, 2.2, and 4.2 by mass). The experimentally tested parameters include load-displacement curves in flexure and uniaxial tension, flexural properties, uniaxial tensile properties, crack development, compressive strength, and drying shrinkage.

RESEARCH SIGNIFICANCE

Even though the concept of ECC is relatively new, its use is gaining acceptance in the construction industry, and it has been successfully used for a number of applications over the last decade. The development of a cost-effective ECC with locally available materials is important for such composite material to be used more commonly in the construction industry in future. Unlike ordinary concrete, standard ECC mixtures have only been produced up to now with commercially available microsilica sand. Commercially available microsilica sand is relatively expensive and difficult to obtain when compared with commonly available sands, such as dolomitic limestone sand and gravel sand; therefore, it is important to investigate how the size and type of commonly available sands influence the mechanical and ductility behavior of ECC. The results reported in this paper show that crushed dolomitic limestone sand and gravel sand can also be successfully used in the production of ECC, and the ductility of the ECC specimens containing crushed sand or gravel sand are comparable with that of standard ECC containing microsilica sand.

EXPERIMENTAL STUDIES

Materials, mixture proportions, and basic mechanical properties

The materials used in the production of standard ECC mixtures were Type I portland cement (C); Class F fly ash (FA) with a calcium content of 5.57%; microsilica sand with an average and maximum grain size of 110 and 200 μm (0.004 and 0.008 in.), respectively; water; polyvinyl alcohol (PVA) fibers; and a polycarboxylic-ether type high-range water-reducing admixture (HRWRA). Chemical composition and physical properties of portland cement and FA are presented in Table 1. Instead of microsilica sand, crushed dolomitic limestone sand of angular particle shape and rounded siliceous gravel fine aggregates with two maximum sizes—that is, 1.19 and 2.38 mm (0.047 and 0.094 in.)—were used in the production of nonstandard ECC mixtures. The particle size distribution of fine aggregates is given in Fig. 2. As seen in Fig. 2, crushed sand (CS) differs from gravel sand (GS) in the grading of fines. The difference is mainly due to the higher amount of very fine particles, that is, particles passing 75 micron (0.003 in.) sieve. The PVA fibers with a diameter of 39 μm (0.002 in.) and a length of 8 mm (0.3 in.) are purposely manufactured with a tensile strength (1620 MPa [235 ksi]), elastic modulus (42.8 GPa [6200 ksi]), and maximum elongation (6.0%) matching those needed for strain-hardening performance. Additionally, the surface of

the PVA fibers is coated with a proprietary oiling agent 1.2% by mass to tailor the interfacial properties between fiber and matrix for strain-hardening performance.[16]

To investigate the influence of aggregate size and type on the mechanical properties of ECC, 15 ECC mixtures having a constant water-cementitious material ratio (*w*/*cm*) of 0.27 were designed. The designation and components of the mixtures are given in Table 2. The variable parameters in these mixtures were the aggregate type, maximum aggregate size (MAS), and FA replacement level (FA/C of 1.2, 2.2, and 4.2 by mass). The amount of cementitious materials (portland cement + FA) and the volume of sand with respect to total volume of the mixture were held constant. All mixtures were prepared using a standard mortar mixer. HRWRA was added to the mixture until the desired fresh ECC characteristics were visually judged acceptable based on past experience; therefore, the HRWRA content was not kept constant. In a control test series, three types of standard ECC mixtures with microsilica sand and an FA/C of 1.2, 2.2, and 4.2 by mass were also studied. As seen from Table 2, the ECC mixture with the lowest FA content (FA/C of 1.2) had the highest HRWRA demand, but as part of the PC was replaced by FA, the HRWRA content of mixtures decreased.

Table 1—Chemical composition and physical properties of portland cement and fly ash

Chemical composition, %	Cement	Fly ash
CaO	61.80	5.57
SiO_2	19.40	59.50
Al_2O_3	5.30	22.20
Fe_2O_3	2.30	3.90
MgO	0.95	—
SO_3	3.80	0.19
K_2O	1.10	1.11
Na_2O	0.20	2.75
Loss on ignition	2.10	0.21
Physical properties		
Specific gravity	3.15	2.18
Retained on 45 μm (0.002 in.), %	12.9	9.6
Water requirement, %	—	93.4

As shown in Table 2, the ECC mixtures are labeled such that the ingredients are identifiable from their IDs. The first two letters in the mixture designations indicate the aggregate type (SS = microsilica sand, CS = crushed sand, and GS = gravel sand). The number after the first two letters indicates the FA/C by mass, and the last number indicates the maximum sand size in mm. For example, the designation "CS_2.2_1.19" identifies ECC mixture with maximum size of 1.19 mm (0.047 in.) crushed sand (CS) and an FA/C of 2.2 by mass.

From each mixture, six 50 mm (2 in.) cubic specimens were prepared for the compressive strength test, eight 203.2 x 76.2 x 12.7 mm (8.0 x 3.0 x 0.5 in.) coupon specimens were prepared for the direct tensile test, and eight 355.6 x 50.8 x 76.2 mm (14 x 2 x 3 in.) prism specimens were prepared for the four-point bending test. All specimens were demolded at the age of 24 hours and moist cured in a plastic bag at 95 ± 5% relative humidity (RH), 23 ± 2 °C (73.4 °F) for 7 days. The specimens were then air cured in laboratory medium at 50 ± 5% RH, 23 ± 2 °C (73.4 °F) until the age of 28 days. Drying shrinkage measurements were also made on ECC mixtures with FA/C of 1.2 and 2.2. The drying shrinkage of three 285 x 25 x 25 mm (11.25 x 1.00 x 1.00 in.) bars was measured up to 90 days after an initial curing of 1 day in the mold and 27 days in lime-saturated water in accordance with ASTM C157 for all ECC mixtures. The drying shrinkage

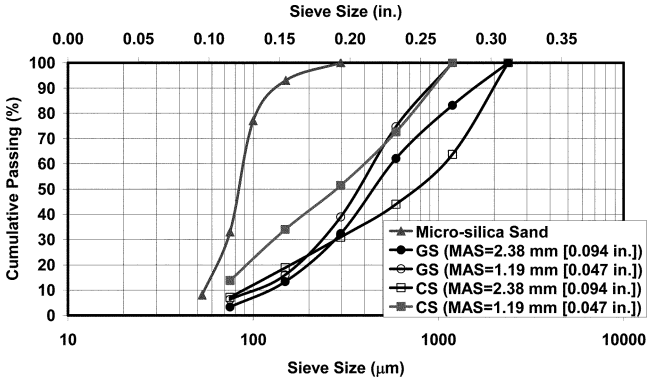

Fig. 2—Sieve analysis of crushed dolomitic limestone sand, gravel sand, and microsilica sand.

Table 2—Mixture properties of ECC

Sand type	Mixture ID	Ingredients, kg/m^3 (lb/yd^3)						FA/C	*w*/*cm*	Compressive strength at 28 days, MPa (ksi)
		C	FA	Water	PVA	Sand	HRWRA			
Silica sand 0.20 mm	SS_1.2_0.20	558 (940)	669 (1127)	326 (549)	26 (44)	446 (751)	2.30 (3.9)	1.20	0.27	62.5 (9.06)
	SS_2.2_0.20	375 (632)	823 (1387)	318 (536)	26 (44)	435 (733)	2.00 (3.4)	2.20	0.27	54.1 (7.85)
	SS_4.2_0.20	217 (366)	957 (1613)	312 (526)	26 (44)	426 (718)	1.60 (2.7)	4.40	0.27	36.8 (5.34)
Crushed sand 1.19 mm	CS_1.2_1.19	559 (942)	671 (1131)	327 (551)	26 (44)	446 (751)	3.20 (5.4)	1.20	0.27	58.4 (8.47)
	CS_2.2_1.19	376 (634)	825 (1390)	319 (538)	26 (44)	436 (735)	2.80 (4.7)	2.20	0.27	46.2 (6.70)
	CS_4.2_1.19	218 (367)	959 (1616)	313 (527)	26 (44)	427 (719)	2.00 (3.4)	4.40	0.27	33.5 (4.86)
Crushed sand 2.38 mm	CS_1.2_2.38	559 (942)	671 (1131)	327 (551)	26 (44)	447 (753)	3.10 (5.2)	1.20	0.27	57.8 (8.38)
	CS_2.2_2.38	376 (634)	825 (1390)	319 (538)	26 (44)	436 (735)	2.30 (3.9)	2.20	0.27	43.4 (6.29)
	CS_4.2_2.38	218 (367)	959 (1616)	313 (527)	26 (44)	427 (719)	1.70 (2.9)	4.40	0.27	31.1 (4.51)
Gravel sand 1.19 mm	GS_1.2_1.19	559 (942)	671 (1131)	327 (551)	26 (44)	447 (753)	2.40 (4.0)	1.20	0.27	58.8 (8.53)
	GS_2.2_1.19	376 (634)	826 (1392)	319 (538)	26 (44)	436 (735)	1.90 (3.2)	2.20	0.27	49.7 (7.21)
	GS_4.2_1.19	218 (367)	959 (1616)	313 (527)	26 (44)	447 (753)	1.70 (2.9)	4.40	0.27	30.6 (4.44)
Gravel sand 2.38 mm	GS_1.2_2.38	559 (942)	671 (1131)	327 (551)	26 (44)	447 (753)	2.30 (3.9)	1.20	0.27	59.0 (8.56)
	GS_2.2_2.38	376 (634)	826 (1392)	319 (538)	26 (44)	436 (735)	1.80 (3.0)	2.20	0.27	42.6 (6.18)
	GS_4.2_2.38	218 (367)	959 (1616)	313 (527)	26 (44)	447 (753)	1.60 (2.7)	4.40	0.27	30.5 (4.42)

specimens were stored in a laboratory at 23 ± 2 °C (73.4 °F), and 50 ± 4% RH.

Direct tensile tests were conducted using an MTS machine with 25 kN (5.62 kip) capacity under displacement control at a rate of 0.005 mm/s (0.0002 in./s). Prior to testing, aluminum plates were glued to both ends of the coupon specimen to facilitate gripping. After direct tensile test, all residual crack widths were measured on the surface of the specimens using a portable microscope. The term "residual crack width" indicates that the crack width is measured from the unloaded specimen after the uniaxial tensile test. Four-point bending test was performed under displacement control at a loading rate of 0.005 mm/s (0.0002 in./s) on a closed-loop controlled servo-hydraulic material test system. The span length of flexural loading was 304.8 mm (12 in.) with a 101.6 mm (4 in.) center span length. During the flexural tests, the load and the midspan deflection were recorded on a computerized data recording system.

RESULTS AND DISCUSSIONS

Compressive strength

The 28-day compressive strength test results of the ECC mixtures incorporating different sand sizes and types, and FA contents are summarized in Table 2. As seen from Table 2 and as expected, the compressive strength of ECC mixtures decreased with increasing FA content. However, even at approximately 80% replacement of cement by FA (FA/C = 4.2), the compressive strength at 28 days of ECC can still exceed that of normal concrete (30 MPa [4.35 ksi]).

At each FA replacement level, ECC mixtures with microsilica sand (SS_1.2_0.20, SS_2.2_0.20, and SS_4.2_0.20) yielded slightly higher compressive strengths than those with gravel sand and crushed sand. In the case of normal concrete, because the surface texture is partly responsible for the bond between paste and aggregate, the crushed sand is expected to produce a better bond between paste and aggregate, and therefore higher compressive strength compared with gravel. However, as seen from Table 2, the two aggregates, that is, crushed sand and gravel sand, produced almost similar compressive strengths and lower than that for ECC mixtures with microsilica sand. Therefore, unlike conventional concrete, aggregate characteristics, such as the surface texture and MAS, did not influence the compressive properties in the case ECC. In general, everything else being the same, the larger the aggregate size, the higher the local *w/c* in the interfacial transition zone and, consequently, the weaker the concrete.[17] The results obtained also indicate that increasing the maximum size of aggregate from 1.19 to 2.38 mm (0.047 to 0.094 in.) for the different sands does not lead to a significant change in the ECC compressive strength. Therefore, it could be stated that, beyond a certain surface area-mass ratio, the particle size of aggregate may not have an important influence on the compressive strength of ECC.

Uniaxial tensile performance of ECC

The uniaxial tensile test results in terms of ultimate tensile strength, ultimate tensile strain at the peak stress, and residual crack width of the newly developed ECC mixtures containing microsilica sand, and crushed sand and gravel sand with a nominal maximum aggregate size of 1.19 mm or 2.38 mm (0.047 in. or 0.094 in.) at 28 days, are displayed in Table 3, and the typical stress-strain curves are presented in Fig. 3. Each data point is an average of at least four uniaxial tensile test results. As seen from the Table 3 and Fig. 3, all

Table 3—Uniaxial tensile properties of ECC specimens at 28 days

Sand type	Mixture ID	Tensile strain, %	Tensile strength, MPa (ksi)	Residual crack width, μm (in.)
Silica sand 0.20 mm	SS_1.2_0.20	2.09 ± 0.16	5.13 ± 0.31l (0.74 ± 0.04)	~60 (0.002)
	SS_2.2_0.20	2.99 ± 0.37	4.59 ± 0.28 (0.67 ± 0.04)	~54 (0.002)
	SS_4.2_0.20	3.21 ± 0.27	3.57 ± 0.12 (0.52 ± 0.02)	~48 (0.002)
Crushed sand 1.19 mm	CS_1.2_1.19	1.96 ± 0.08	4.75 ± 0.40 (0.69 ± 0.06)	~59 (0.002)
	CS_2.2_1.19	2.62 ± 0.68	4.14 ± 0.25 (0.60 ± 0.04)	~57 (0.002)
	CS_4.2_1.19	3.04 ± 0.67	4.65 ± 0.27 (0.67 ± 0.04)	~50 (0.002)
Crushed sand 2.38 mm	CS_1.2_2.38	2.34 ± 0.21	5.02 ± 0.22 (0.73 ± 0.03)	~57 (0.002)
	CS_2.2_2.38	2.47 ± 0.18	4.19 ± 0.27 (0.61 ± 0.04)	~54 (0.002)
	CS_4.2_2.38	2.76 ± 0.24	3.57 ± 0.13 (0.52 ± 0.02)	~45 (0.002)
Gravel sand 1.19 mm	GS_1.2_1.19	1.99 ± 0.16	4.84 ± 0.33 (0.70 ± 0.05)	~55 (0.002)
	GS_2.2_1.19	2.19 ± 0.24	4.44 ± 0.37 (0.64 ± 0.05)	~50 (0.002)
	GS_4.2_1.19	3.23 ± 0.77	3.58 ± 0.42 (0.52 ± 0.06)	~45 (0.002)
Gravel sand 2.38 mm	GS_1.2_2.38	2.08 ± 0.28	4.46 ± 0.36 (0.65 ± 0.05)	~53 (0.002)
	GS_2.2_2.38	2.49 ± 0.37	4.00 ± 0.15 (0.58 ± 0.02)	~54 (0.002)
	GS_4.2_2.38	3.12 ± 0.77	3.65 ± 0.24 (0.53 ± 0.03)	~45 (0.002)

ECC specimens show strain-hardening behavior, that is, a sustained increase in load capacity beyond the first matrix crack, with strain capacities from 1.96% to more than 3.00%, which are in the range of 190 to 300 times the ductility of conventional concrete and normal fiber-reinforced concrete. The first-crack strengths decrease from 4.0 to 3.0 MPa with the increase of the FA/C from 1.2 to 4.2. After the first cracking, the load continues to increase accompanied by multiple cracking, which contributes to the inelastic strain as stress increases.

According to micromechanical principles, the satisfaction of two conditions is necessary to achieve strain-hardening behavior.[1] First, the crack tip toughness $J_{tip}(K_m/E_m)$ should be less than the complementary energy J_b', calculated from the bridging stress-versus-crack opening curve.

$$J_b' = \sigma_0\delta_0 - \int_0^{\delta_0}\sigma(\delta)d\delta \geq J_{tip} \approx \frac{K_m^2}{E_m} \quad (1)$$

where σ_0 and δ_0 are the maximum crack bridging stress and corresponding crack opening, respectively; K_m is the fracture toughness of the mortar matrix; and E_m is the elastic modulus of the mortar matrix. Second, the tensile first-crack strength σ_{fc} must not exceed the maximum bridging stress σ_0 ($\sigma_0 > \sigma_{fc}$). A lower tensile first-crack strength and lower matrix toughness is therefore favorable for strain-hardening behavior.

Tensile ductility of ECC mixtures for different aggregate types and sizes is plotted against FA content and illustrated in Fig. 4. As can be seen from Fig. 4, the increase of FA/C

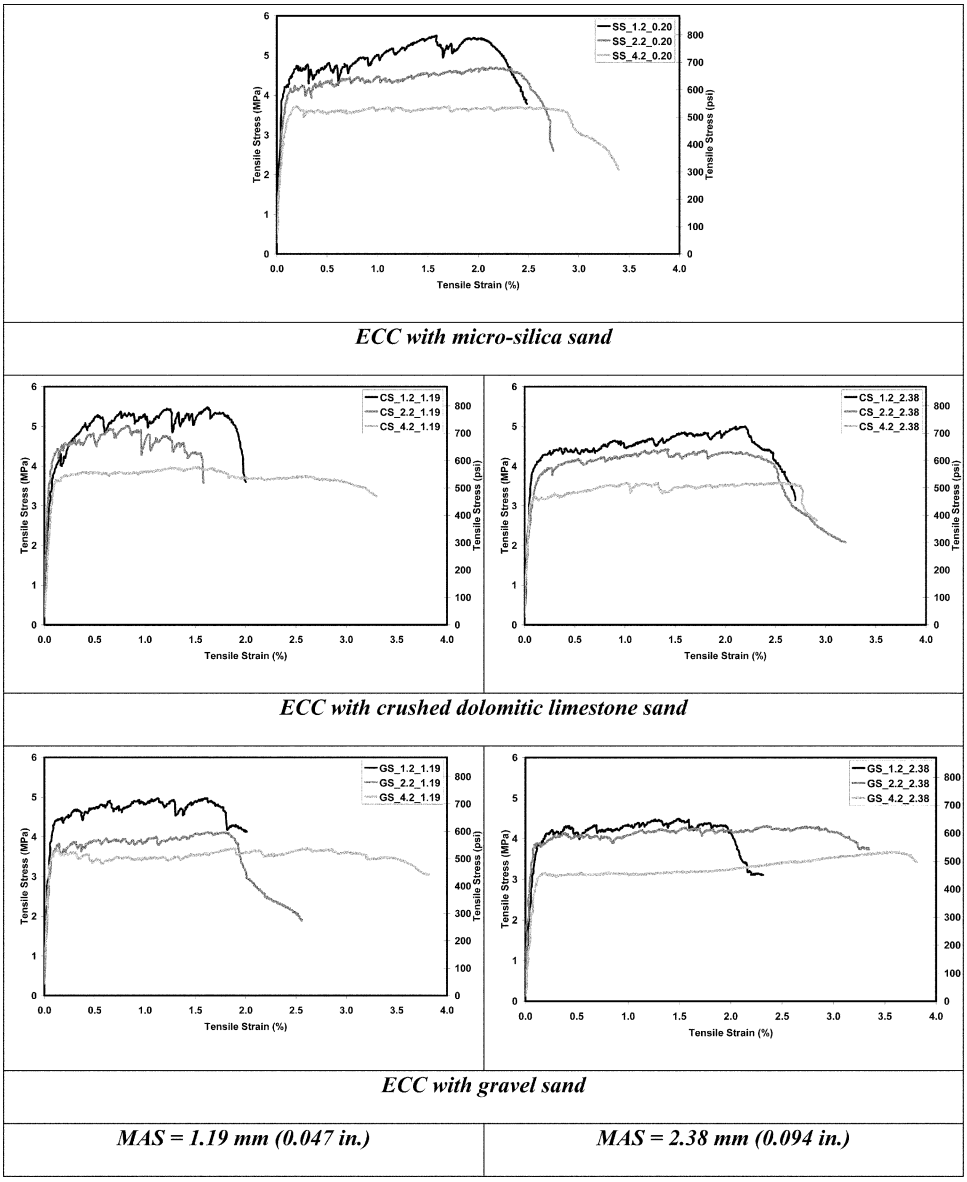

Fig. 3—Typical tensile stress-tensile strain curves of ECC mixtures at age of 28 days.

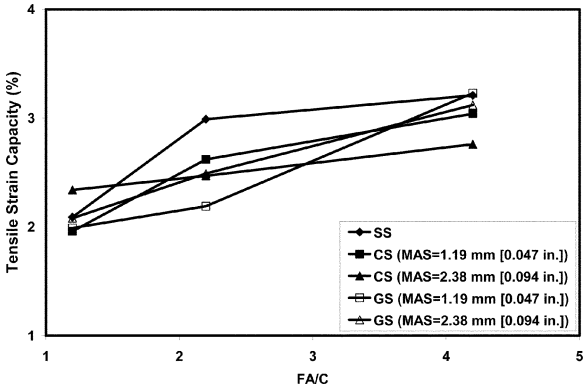

Fig. 4—Tensile strain capacity of ECC as function of FA/C for different aggregate types and size.

increases the tensile strain capacity of ECC at 28 days of age. Particularly, for all ECC mixtures, the strain capacities of ECC mixtures with an FA/C of 4.2 were found to be significantly greater than those with lower FA/C. The increase in the tensile strain with the increase in the FA content can be attributed to the fact that the increase in the FA content tends to reduce the PVA fiber/matrix interface chemical bond and matrix toughness, while increasing the interface frictional bond, in favor of attaining high tensile strain capacity.[14] On the other hand, the increase in the FA content significantly reduced the tensile strength. For all aggregate types, ECC specimens with FA/C of 1.2 exhibits a significantly higher ultimate tensile strength (up to 30% higher, depending on the FA/C), whereas the ECC specimens with higher FA content (especially FA/C of 4.2) exhibit more ductile behavior.

As seen from Table 3, the ductility and tensile strength of the ECC mixtures with crushed sand and gravel sand are comparable with that of standard ECC specimens with microsilica sand. These ECC composites exhibited a strain capacity from 1.96 to 3.23% at 28 days of age. The tensile strain capacity is generally observed to be slightly higher for gravel sand than for crushed sand with the same size of aggregate. This might be attributed to the difference in the bond strength between the matrix and aggregate, and hence the toughness of ECC matrix with crushed aggregates will be higher due to the superior bond between the crushed sand

and paste. Therefore, in addition to FA replacement level, the results presented herein indicate that tensile ductility is dependent on the aggregate characteristics, such as the surface texture. The surface roughness of aggregate strongly influences the overall behavior of the normal concrete, that is, the matrix toughness with crushed aggregate is generally higher than that with natural aggregate.[12]

The typical tensile stress-tensile strain curves of ECC specimens containing different maximum aggregate sizes are shown in Fig. 3. As seen from Fig. 3, the effects of increasing the maximum size of aggregate from 1.19 mm to 2.38 mm (0.047 in. to 0.094 in.) (regardless of sand type) on the shape of stress-strain curves, tensile strain, and tensile strength of ECC specimens are fairly small, which is surprising. This result was also consistent with the later results of flexural test results of ECC specimens. It is well known that increasing aggregate size generally produces higher fracture energy for plain concrete and, therefore, higher matrix toughness,[13] which is expected to contribute to a reduction in tensile strain capacity according to micromechanics theory of ECC explained previously. The reason for remarkable tensile strain even with conventional sands of 2.38 mm (0.094 in.) Maximum aggregate size (MAS) may be attributed to the use of high volumes of FA in the production of ECC. In the literature, it was discovered that FA possesses a number of remarkable advantageous effects to ECC development. Specifically, the micromechanics study showed that the presence of FA reduced the fiber/matrix interfacial chemical bond while simultaneously lowering the matrix toughness, thus improving strain-hardening potential.[14] Another possible explanation is that a partial replacement of cement by FA results in a higher volume of paste at constant total weight of cementitious materials due to its lower density, and this increase in the paste volume reduces the friction at the fine aggregate-paste interface and improves the plasticity and cohesiveness;[18,19] this leads to a better distribution of the fibers in the mortar matrix. Moreover, the spherical shape of FA reduces the friction at the aggregate-paste interface, producing a "ball-bearing effect" at the point of contact,[20,21] which might also improve the distribution of fibers. As a result, ductility appears to be independent of aggregate size at a given aggregate content, at least within the size range studied herein.

Table 3 summarizes the effect of aggregate type and size, and FA replacement level on the residual crack width at different ages. After unloading, multiple microcracks with a small average crack width and fine crack spacing were observed (Fig. 5(a)). It was also found that the crack width reduces slightly as FA content increases. On the other hand, the use of crushed sand and gravel sand up to 2.38 mm (0.094 in.) MAS did not influence the average residual crack width, and it is less than 60 μm (0.002 in.) for all ECC mixtures studied. Crack width control is of primary importance for many reinforced concrete applications because it is believed that there is a close relationship between the mean or maximum crack widths and the durability of the structure. Moreover, the lower magnitude of the crack width is expected to promote self-healing behavior and, thus, the transport properties in cracked composites.[5,8,22,23] Consequently, in the serviceability limit state, a mean or maximum crack width less than approximately 0.1 mm (0.004 in.) is usually prescribed.[24,25]

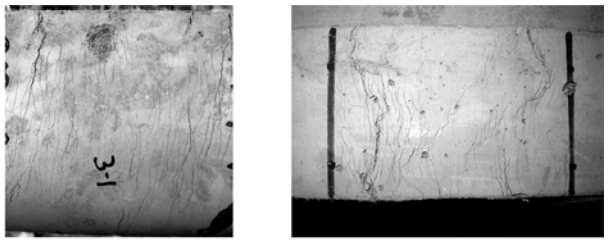

(a) after uniaxial tensile (Mix ID.: CS_4.2_1.19) (b) after flexure load (Mix ID.: GS_2.2_2.38)

Fig. 5—Typical crack pattern on surface of ECC coupon and beam specimens after uniaxial tensile and flexure load applications.

Flexural performance of ECC

The test results in terms of flexural strength (modulus of rupture [MOR]) and ultimate midspan deflection at the peak stress are displayed in Table 4, and the typical flexural stress-midspan deflection curves for different aggregate types and sizes, and FA replacement levels of the ECC mixtures are shown in Fig. 6. To facilitate the comparison between the test results for different ECC mixtures, the same scales for both axes were used in this figure. Each result in Table 4 is the average of four to six specimens.

Typical behavior of ECC beams with gravel sand under four-point bending load is shown in Fig. 7. As seen from the figure, under severe bending load, an ECC beam containing normal sand up to 2.38 mm (0.094 in.) MAS deforms similarly to a ductile metal plate through plastic deformation (Fig. 7). In all of the ECC specimens, the first crack started inside the midspan at the tensile face. The flexural stress increases at a slower rate along with the development of multiple cracks

Table 4—Flexural properties of ECC specimens at 28 days

Sand type	Mixture ID	Ultimate deflection, mm (in.)	Flexural strength, MPa (psi)
Silica sand 0.20 mm	SS_1.2_0.20	4.51 ± 0.47 (0.178 ± 0.019)	12.12 ± 0.86 (1.76 ± 0.12)
	SS_2.2_0.20	4.56 ± 0.05 (0.180 ± 0.002)	11.48 ± 0.92 (1.67 ± 0.13)
	SS_4.2_0.20	6.31 ± 1.01 (0.248 ± 0.04)	8.67 ± 0.75 (1.26 ± 0.11)
Crushed sand 1.19 mm	CS_1.2_1.19	3.92 ± 0.59 (0.154 ± 0.023)	11.71 ± 1.24 (1.70 ± 0.18)
	CS_2.2_1.19	3.97 ± 0.08 (0.156 ± 0.003)	11.17 ± 0.42 (1.62 ± 0.06)
	CS_4.2_1.19	5.22 ± 0.61 (0.206 ± 0.024)	8.98 ± 1.07 (1.30 ± 0.16)
Crushed sand 2.38 mm	CS_1.2_2.38	3.19 ± 0.82 (0.126 ± 0.032)	12.46 ± 0.19 (1.81 ± 0.03)
	CS_2.2_2.38	4.66 ± 0.87 (0.183 ± 0.034)	11.29 ± 2.15 (1.64 ± 0.31)
	CS_4.2_2.38	4.71 ± 0.26 (0.185 ± 0.010)	8.14 ± 0.54 (1.18 ± 0.04)
Gravel sand 1.19 mm	GS_1.2_1.19	4.04 ± 0.28 (0.159 ± 0.011)	12.75 ± 2.23 (1.85 ± 0.32)
	GS_2.2_1.19	4.58 ± 0.46 (0.180 ± 0.018)	10.60 ± 1.63 (1.54 ± 0.24)
	GS_4.2_1.19	6.51 ± 0.40 (0.256 ± 0.016)	9.62 ± 1.72 (1.40 ± 0.25)
Gravel sand 2.38 mm	GS_1.2_2.38	4.00 ± 0.42 (0.157 ± 0.017)	11.56 ± 1.35 (1.68 ± 0.20)
	GS_2.2_2.38	4.48 ± 0.22 (0.176 ± 0.009)	9.72 ± 0.64 (1.41 ± 0.09)
	GS_4.2_2.38	5.09 ± 0.43 (0.200 ± 0.017)	9.19 ± 2.00 (1.33 ± 0.29)

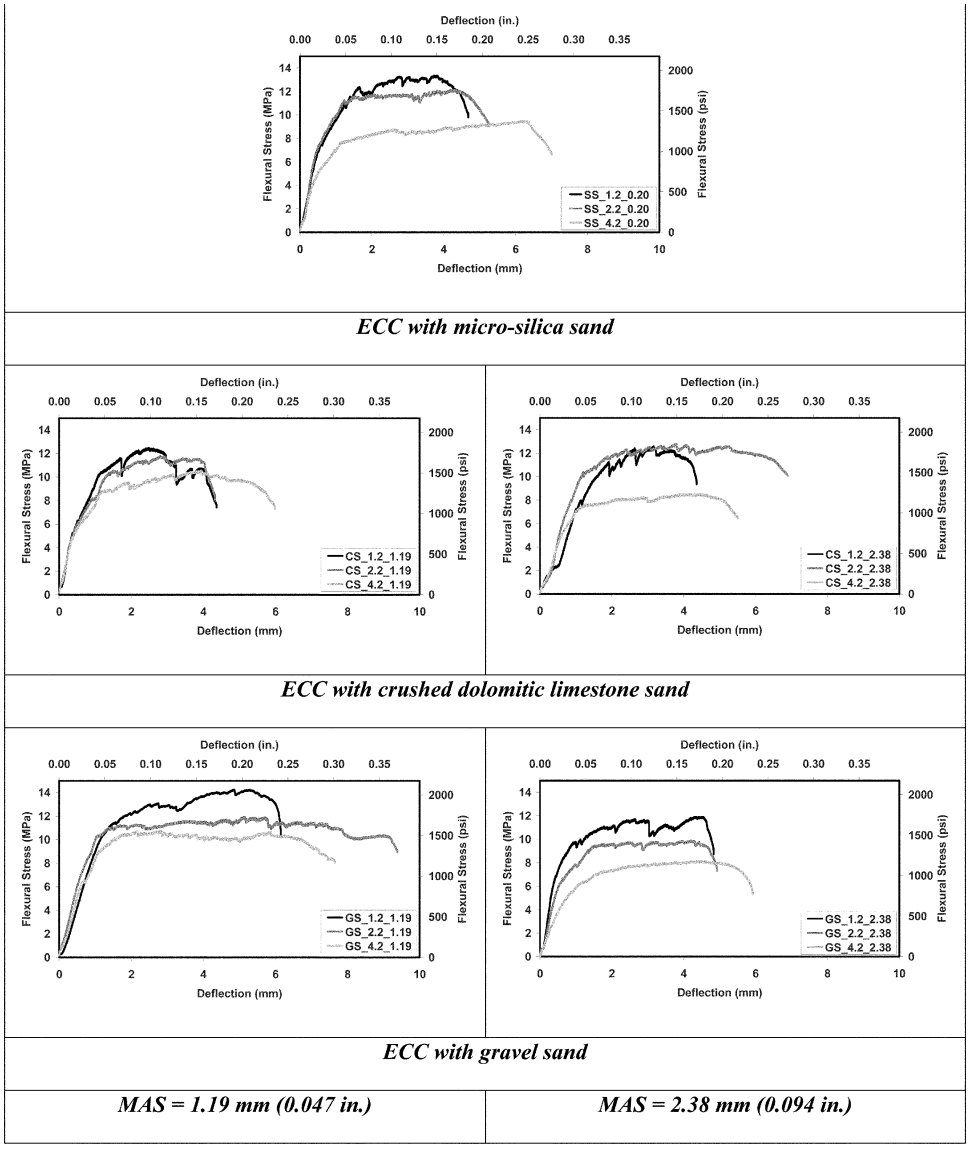

Fig. 6—Typical flexural stress-midspan deflection curves of ECC mixtures at age of 28 days.

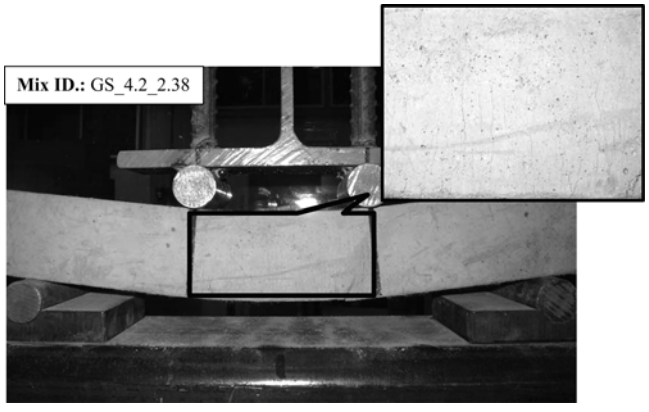

Fig. 7—Response of ECC beams under four-point flexural loading.

with small crack spacing and tight crack widths (<0.1 mm [0.004 in.]). Microcracks developed from the first cracking point and spread out in the midspan of the flexural beam, as shown in Fig. 5(b). Bending failure in ECC occurred when the fiber-bridging strength at one of the microcracks was reached, resulting in localized deformation at this section (Fig. 5(b)) once the MOR is approached.

As seen from Table 4, the averaged ultimate flexural strengths vary from 8.14 to 12.75 MPa (1.18 to 1.85 ksi) depending on the FA replacement level. For example, the flexural strength of ECC with an FA/C of 4.2 is approximately 65% that of the ECC mixtures with an FA/C of 1.2. The MOR is likely limited by the fiber-bridging capacity governed by the fiber/matrix bond and, in turn, by the FA/C. However, even at approximately 80% replacement of cement by FA (FA/C = 4.2), the flexural strength of ECC at 28 days was not significantly different from that of fiber-reinforced concrete. As in the case of uniaxial tensile strength results, the aggregate type and size, on the other hand, have only a minor effect on the flexural strengths.

The total deflection of ECC beam, which reflects the material ductility, strongly depends on the amount of FA content (Table 4). The total deflection increases as the replacement level of FA increases, reaching as much as 6.51 mm (0.256 in.) at peak load. Among the ECCs having an FA/C of 1.2, the highest midspan deflection (4.51 mm [0.178 in.]) was

observed for specimens containing microsilica sand. When the FA/C was increased, however, ECC mixtures with crushed sand and gravel sand showed similar or higher deflection capacity than that of ECC mixtures with microsilica sand. For example, the beam deflection at peak stress of the ECC mixtures with gravel sand (1.19 mm [0.047 in.] of MAS) at FA/C of 2.2 and 4.2 is higher than those of microsilica sand ECC mixtures (Table 4). As with tensile strain, for both aggregate sizes, the gravel sand provided higher values for the midspan deflection than the crushed limestone (up to 20% greater), especially at higher cement replacement levels. This could be attributed to a greater aggregate-paste bond in the case of crushed sand compared to gravel sand, and therefore higher matrix toughness at a given aggregate content.[26]

The increase in MAS slightly damages the ductility characteristics, total midspan beam deflection, of ECC. The negative effects of increasing aggregate size on ductility may be attributed to the adverse effect on the uniform dispersion of fibers. The balling of fibers encouraged by coarser sands at constant sand content prevents sufficient coating of fibers by the matrix, and thus reduces the fiber-to-matrix bonding, which is an important factor influencing ductility. Moreover, for ECC with the larger aggregate, a higher degree of aggregate interlock is expected, resulting in higher matrix toughness and work-of-fracture during crack propagation.

As shown in Fig. 6, the initial slopes of the load-deflection curves for all ECC mixtures containing different aggregate types and sizes at constant FA content are practically identical. The slope of the load-deflection curve represents the stiffness of the beams, and it can be easily noted from Fig. 6 that the slope decreases with increasing FA content, thereby indicating a reduction in the stiffness of the ECC beams. The first crack load was defined as the load at which the load-deformation response deviated from linearity. For all ECC mixtures, the first crack load increases up to approximately 70% of the peak load for fiber composites. The increase in FA/C from 1.2 to 4.2 also reduces the first crack strength by an average of 20%. Figure 6 shows, however, that aggregate type and MAS have little influence on the magnitude of the first crack loads and stiffness of the ECC beams at constant FA/C.

Drying shrinkage

The results of drying shrinkage test at the age of 90 days are shown in Fig. 8. Each value in Fig. 8 represents the average drying-shrinkage measurements of three specimens. The ECC mixtures produced for this study had the same *w*/*cm*, so varying water requirement was not a factor for drying shrinkage. The drying shrinkage strains at the age of 90 days ranged between 701 and 1698 microstrain. ECC mixtures with an FA/C of 1.2 and microsilica sand (SS_1.2_0.20) exhibited the highest drying shrinkage of 1698 microstrain at the end of 90 days. The general trend in Fig. 8 shows that the increase in the FA content, especially in the case of ECC mixtures containing microsilica sand, can effectively reduce free drying-shrinkage deformation. Similar results have been reported for high-volume fly ash (HVFA) concrete.[27] In the present study, a reduction up to 20% of drying shrinkage, depending on the aggregate type, was found when the FA/C was increased from 1.2 to 2.2. A possible mechanism contributing to the reduction of drying shrinkage in ECCs is the matrix densification due to FA addition, which may prevent internal moisture evaporation.[28] The matrix densification is typically attributed to the shape, pozzolanic property, and micro-filler effect of FA. An alternative mechanism is that unhydrated FA particles serve as fine aggregates to restrain the shrinkage deformation.[27,29,30]

From this experimental study, it is apparent that the increase in size of aggregate significantly reduces the long-term drying shrinkage. The drying shrinkage of ECC, at the age of 90 days, slightly decreases with the increase of MAS from 1.19 mm to 2.38 mm. The reduced values of drying shrinkage with the addition of larger-size aggregates are due primarily to the restraining action of the aggregate in the mortar. The results also showed that the restraining effect of the microsilica sand in the ECC mixtures was too small to contribute significantly to drying shrinkage. Among the ECC mixtures studied in this study, crushed sand ECC mixtures exhibited the lowest shrinkage values. This could be explained by the superior bond in crushed sand ECC compared to gravel ECC, due to aggregate shape and surface texture that may prevent internal moisture evaporation.

CONCLUSIONS

This paper described the influence of aggregate size and type on the mechanical performances of ECC with three different FA contents. Aggregates from two sources were used: a crushed dolomitic limestone sand and gravel sand. In addition, standard ECC mixtures with microsilica sand were produced for control purposes. A series of tests were carried out to study the compressive, uniaxial tensile, flexure, and shrinkage properties of ECC. The test results indicate that aggregates within the size range studied, as long as they do not interfere with the uniform dispersion of fibers, do not negatively influence the ductility of ECC. The negative effects of aggregates on fiber dispersion and matrix toughness can be eliminated or minimized by increasing FA content (replacing cement). For all aggregate types, ECC specimens with an FA/C of 1.2 exhibit significantly higher ultimate tensile, flexural, and compressive strengths, whereas the ECC specimens with higher FA content (especially FA/C of 4.2) exhibit more ductile behavior. This was true for all aggregate types and sizes used in the production of ECC in this study. On the other hand, the ductility and strength properties of ECCs are minorly or not affected by increasing the maximum size of aggregate. The use of crushed sand and gravel sand with higher MAS can also reduce drying shrinkage, further improving the material behavior.

Finally, the results presented in this study provide a preliminary database for the suitability of crushed sand and gravel sand in the production of ECC, and indicate that crushed sand and gravel sand with relatively higher nominal

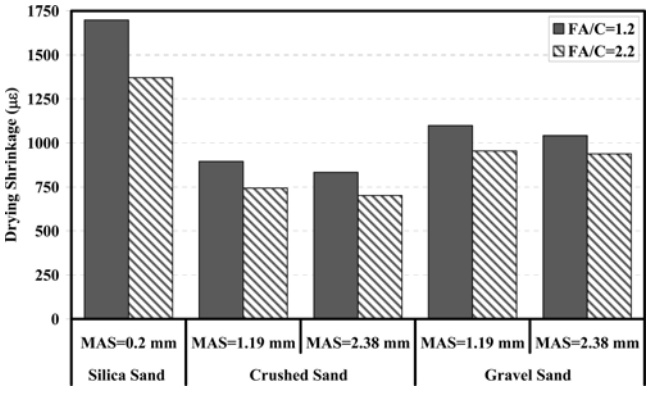

Fig. 8—Drying shrinkage of ECC mixtures at 90 days.

aggregate size can also be successfully used to produce an ECC having similar or better mechanical properties than corresponding ECC made with microsilica sand. For a complete understanding of ductility and mechanical performances of ECC containing crushed sand and gravel sand with different maximum aggregate size, further research will be needed on a micromechanical scale to determine changes of ECC matrix toughness and fiber/matrix interface properties. Further, due to the prolonged pozzolanic reaction of FA, it would be necessary to investigate the long-term behavior (beyond 28 days) of ECC with larger MAS and high FA content.

ACKNOWLEDGMENTS

The authors gratefully acknowledge the financial assistance of the Natural Sciences and Engineering Research Council (NSERC) of Canada, the Canada Research Chair Program, and the Scientific and Technical Research Council (TUBITAK) of Turkey provided under Project: MAG-108M495. Support from the U.S. National Science Foundation (NSF CI-Team OCI 0636300) for international collaborative research on ECC is gratefully acknowledged.

REFERENCES

1. Li, V. C., "ECC—Tailored Composites through Micromechanical Modeling," *Fiber Reinforced Concrete: Present and the Future*, N. Banthia et al., eds., CSCE, Montreal, QC, Canada, 1998, pp. 64-97.

2. Li, V. C., "On Engineered Cementitious Composites (ECC)—A Review of the Material and its Applications," *Advanced Concrete Technology*, V. 1, No. 3, 2003, pp. 215-230.

3. Li, V. C.; Wang, S.; and Wu, C., "Tensile Strain-Hardening Behavior of PVA-ECC," *ACI Materials Journal*, V. 98, No. 6, Nov.-Dec. 2001, pp. 483-492.

4. Sahmaran, M., and Li, V. C., "De-icing Salt Scaling Resistance of Mechanically Loaded Engineered Cementitious Composites," *Cement and Concrete Research*, V. 7, No. 37, 2007, pp. 1035-1046.

5. Sahmaran, M.; Li, V. C.; and Li, M., "Transport Properties of Engineered Cementitious Composites under Chloride Exposure," *ACI Materials Journal*, V. 104, No. 6, Nov.-Dec. 2007, pp. 604-611.

6. Sahmaran, M., and Li, V. C., "Durability of Mechanically Loaded Engineered Cementitious Composites under High Alkaline Environment," *Cement and Concrete Composites*, V. 30, No. 2, 2008, pp. 72-81.

7. Sahmaran, M.; Li, V. C.; and Andrade, C., "Corrosion Resistance Performance of Steel-Reinforced Engineered Cementitious Composite Beams," *ACI Materials Journal*, V. 105, No. 3, May-June 2008, pp. 243-250.

8. Sahmaran, M., and Li, V.C., "Influence of Microcracking on Water Absorption and Sorptivity of ECC," *Materials and Structures*, DOI 10.1617/s11527-008-9406-6, July 2008.

9. Li, M.; Sahmaran, M.; and Li V.C., "Effect of Cracking and Healing on Durability of Engineered Cementitious Composites under Marine Environment," *High Performance Fiber Reinforced Cement Composites (HPFRCC-5)*, Stuttgart, Germany, V. 10-13, 2007, pp. 313-322.

10. De Koker, D., and van Zijl, G., "Extrusion of Engineered Cement-Based Composite Material," *Proceedings of BEFIB*, Varenna, Lake Como, Italy, Sept. 2004, pp. 1301-1310.

11. Soroushian, P.; Nagi, M.; and Hsu, J., "Optimization of the Use of Lightweight Aggregates in Carbon Fiber Reinforced Cement," *ACI Materials Journal*, V. 89, No. 3, May-June 1992, pp. 267-276.

12. Nallthambi, P.; Karihaloo, B.; and Heaton, B., "Effect of Specimen and Crack Sizes, Water/Cement Ratio and Coarse Aggregate Texture upon Fracture Toughness of Concrete," *Magazine of Concrete Research*, V. 36, No. 129, 1984, pp. 227-236.

13. Perdikaris, P. C., and Romeo, A., "Size Effect on Fracture Energy of Concrete and Stability Issues in Three-Point Bending Fracture Toughness Testing," *ACI Materials Journal*, V. 92, No. 5, Sept.-Oct. 1995, pp. 483-496.

14. Wang, S., and Li, V. C., "Engineered Cementitious Composites with High-Volume Fly Ash," *ACI Materials Journal*, V. 104, No. 3, May-June 2007, pp. 233-241.

15. Yang, E. H.; Yang, Y.; and Li, V. C., "Use of High Volumes of Fly Ash to Improve ECC Mechanical Properties and Material Greenness," *ACI Materials Journal*, V. 104, No. 6, Nov.-Dec. 2007, pp. 620-628.

16. Li, V. C.; Wu, C.; Wang, S.; Ogawa, A.; and Saito, T., "Interface Tailoring for Strain-Hardening PVA-ECC," *ACI Materials Journal*, V. 99, No. 5, Sept.-Oct. 2002, pp. 463-472.

17. Mehta, P. K., and Monteiro, P. J. M., *Concrete: Structure, Properties, and Materials*, Third Edition, McGraw Hill, New York, 2006, 659 pp.

18. Sahmaran, M.; Christianto, H. A.; and Yaman I. O., "The Effect of Chemical Admixtures and Mineral Additives on the Properties of Self-Compacting Mortars," *Cement and Concrete Composites*, V. 28, No. 5, 2006, pp. 432-440.

19. ACI Committee 232, "Use of Natural Pozzolans in Concrete," *ACI Materials Journal*, V. 91, No. 4, July-Aug. 1994, pp. 410-426.

20. Wei, S.; Handong, Y.; and Binggen, Z., "Analysis of Mechanism on Water-Reducing Effect of Fine Ground Slag, High-Calcium Fly Ash, and Low-Calcium Fly Ash," *Cement and Concrete Research*, V. 33, No. 8, 2003, pp. 1119-1125.

21. Okamura, H., and Ouchi, M., "Self-Compacting Concrete," *Journal of Advanced Concrete Technology*, V. 11, No. 1, 2003, pp. 5-15.

22. Lepech, M. D., and Li, V. C., "Water Permeability of Cracked Cementitious Composites," Paper 4539 of Compendium of Papers, ICF 11, Turin, Italy, Mar. 2005. (CD-ROM)

23. Yang, Y.; Lepech, M. D.; and Li, V. C., "Self-Healing of ECC under Cyclic Wetting and Drying," *Proceedings of International Workshop on Durability of Reinforced Concrete under Combined Mechanical and Climatic Loads*, Qingdao, China, 2005, pp. 231-242.

24. Evardsen, C., "Water Permeability and Autogenous Healing of Cracks in Concrete," *ACI Materials Journal*, V. 96, No. 4, July-Aug. 1999, pp. 448-454.

25. Reinhardt, H. W., and Jooss, M., "Permeability and Self-Healing of Cracked Concrete as a Function of Temperature and Crack Width," *Cement and Concrete Research*, V. 33, No. 7, 2003, pp. 981-985.

26. Cetin, A., and Carrasquillo R. L., "High-Performance Concrete: Influence of Coarse Aggregates on Mechanical Properties," *ACI Materials Journal*, V. 95, No. 3, May-June 1998, pp. 252-261.

27. Sahmaran, M.; Yaman I. Ö.; and Tokyay, M., "Development of High Volume Low-Lime and High-Lime Fly-Ash-Incorporated Self Consolidating Concrete," *Magazine of Concrete Research*, V. 59, No. 2, 2007, pp. 97-106.

28. Maslehuddin, M.; Saricimen, H.; and Al-Mani, A., "Effect of Fly Ash Addition on the Corrosion Resisting Characteristics of Concrete," *ACI Materials Journal*, V. 84, No. 1, Jan.-Feb. 1987, pp. 42-50.

29. Zhang, M. N., "Microstructure, Crack Propagation, and Mechanical Properties of Cement Pastes Containing High Volumes of Fly Ashes," *Cement and Concrete Research*, V. 25, No. 6, 1995, pp. 1165-1178.

30. Bisaillon, A.; Rivest, M.; and Malhotra, V. M., "Performance of High-Volume Fly Ash Concrete in Large Experimental Monoliths," *ACI Materials Journal*, V. 91, No. 2, Mar.-Apr. 1994, pp. 178-187.